Link Level Analysis of NR V2X Sidelink Communications

Luca Lusvarghi, *Associate Member, IEEE*, Baldomero Coll-Perales, *Member, IEEE*, Javier Gozalvez, *Senior Member, IEEE*, and Maria Luisa Merani, *Senior Member, IEEE*

***Abstract*—The Internet of Vehicles (IoV) will interconnect vehicles, vulnerable road users, and infrastructure nodes for a safer, more efficient, and digitalized mobility. In the IoV vision, traditional network-based communications will be complemented with direct sidelink (SL) vehicle-to-everything (V2X) communications. To this aim, third generation partnership project (3GPP) introduced in Release 16 the new radio (NR) V2X SL technology. The NR V2X SL standard includes important physical (PHY)-layer novelties with respect to LTE V2X SL and NR uplink/downlink, and is characterized by a large set of configurable parameters. However, existing NR V2X SL link level (LL) studies focus on a confined set of configurations. This limits a thorough understanding of the NR V2X SL LL performance and impacts the accuracy of system level evaluations, which typically leverage LL models to accurately represent the PHY layer performance. These models are based on look-up tables (LUTs) that map the LL performance, e.g., block error rate (BLER), as a function of the link quality, e.g., signal-to-noise ratio (SNR). This study presents an exhaustive NR V2X SL LL evaluation that analyzes the impact of relevant PHY layer aspects, e.g., modulation and coding scheme, channel model, and transmitter–receiver relative speed, considering the wide set of configurations recommended by 3GPP and European Telecommunications Standards Institute. The obtained standard-compliant LUTs are openly released, representing the largest NR V2X SL LL data set available. The released data set represents a valuable asset for the community, as it allows exhaustive NR V2X SL system level investigations under a broad range of settings and configurations.**

***Index Terms*—5G new radio (NR), block error rate (BLER), C-V2X, link level (LL), look-up tables (LUTs), LUTs, NR V2X, sidelink (SL), system level, vehicle-to-everything (V2X).**

Manuscript received 11 January 2024; revised 15 April 2024; accepted 10 May 2024. Date of publication 17 May 2024; date of current version 23 August 2024. The work of Luca Lusvarghi, Baldomero Coll-Perales, and Javier Gozalvez was supported in part by MCIU/AEI/10.13039/501100011033 under Grant IJC2018-036862-I and Grant PID2020-115576RB-I00; in part by ESF+ under Grant RYC2022-036953-I; and in part by the "European Union NextGenerationEU/PRTR" under Grant TED2021-130436B-I00. The work of Maria Luisa Merani was supported by the FAR Dipartimentale 2021-2022, Università degli Studi di Modena e Reggio Emilia. *(Corresponding author: Luca Lusvarghi.)*

Luca Lusvarghi, Baldomero Coll-Perales, and Javier Gozalvez are with the UWICORE Laboratory, Universidad Miguel Hernández de Elche, 03202 Elche, Spain (e-mail: llusvarghi@umh.es; bcoll@umh.es; j.gozalvez@umh.es).

Maria Luisa Merani is with the Department of Engineering "Enzo Ferrari," Università degli Studi di Modena e Reggio Emilia, 41125 Modena, Italy, and and also with Consorzio Nazionale Interuniversitario per le Telecomunicazioni, 43100 Parma, Italy (e-mail: marialuisa.merani@unimore.it).

Digital Object Identifier 10.1109/JIOT.2024.3402551

I. Introduction

THE Internet of Vehicles (IoV) represents a critical cornerstone in the digitalization of connected and automated mobility, as it will allow connected vehicles to communicate with each other, with vulnerable road users, and with the infrastructure to improve road safety and transportation efficiency. To this end, vehicle-to-everything (V2X) communications will play a critical role, allowing connected vehicles to exchange information and support awareness [1] or enhanced V2X (eV2X) use cases, such as cooperative perception, maneuver coordination, and platooning [2], that exhibit a wide range of latency, reliability, and data rate requirements. To cope with the demanding requirements of eV2X use cases, the third generation partnership project (3GPP) introduced an adaptation of the 5G new radio (NR) standard for V2X sidelink (SL) or direct communications in Release 16. In SL communications, connected vehicles directly exchange information without relaying the data transmission through the cellular infrastructure. The so-called NR V2X SL standard complements (and does not replace) the LTE V2X SL standard published in Release 14 for basic awareness use cases. With respect to LTE V2X SL, NR V2X SL introduces a new Physical (PHY) layer design and new scheduling strategies for a more flexible management of the radio resources. For instance, NR V2X SL features a flexible subcarrier spacing (SCS) configuration, more spectrally efficient modulation and coding schemes (MCSs), and more sophisticated demodulation reference signal (DMRS) patterns. In addition, NR V2X SL exhibits relevant differences at the PHY layer with respect to 5G NR uplink (UL) and downlink (DL) communications [3]. For example, the control information is transmitted in two distinct stages in NR V2X SL, and each stage employs specific encoding and decoding procedures. This is in contrast to 5G UL/DL, where the control information is transmitted in a single stage. Moreover, NR V2X SL employs dedicated procedures to compute the maximum payload size and to encode/decode the payload content. NR V2X SL also defines a dedicated set of DMRS patterns to achieve an improved communication robustness in high-speed mobility vehicular environments.

The introduction of a new PHY layer design mandates for a thorough link level (LL) evaluation to assess the performance of NR V2X SL communications and the Quality of Service (QoS) levels (e.g., the communication range) that can be guaranteed to eV2X applications. A complete LL analysis is

particularly necessary in the case of NR V2X SL, as it is characterized by a large set of configurable parameters. However, existing NR V2X SL LL studies focus on a confined number of configurations, thus limiting a comprehensive understanding of the link-level performance and the achievable QoS levels that characterize NR V2X SL communications. A limited evaluation of NR V2X SL communications at the LL can also impact the accuracy of system level studies. This is the case because system level simulators (also referred to as network level simulators) concentrate on system-related aspects, such as medium access (including the impact of channel load and interference), networking, and user mobility, and do not explicitly model PHY layer aspects in order to confine the simulation complexity and cost. Instead, they leverage LL performance models to accurately represent the effects of the PHY layer. These models typically consist of look-up tables (LUTs) that report the LL performance, e.g., the block error rate (BLER), as a function of the link quality, e.g., the signal-to-noise ratio (SNR). LUTs are obtained with LL simulators that implement the transmitter and receiver chains up to the individual signal samples, i.e., featuring an accurate implementation of all the channel encoding-decoding, channel estimation, modulation-demodulation, data multiplexing–demultiplexing mechanisms. LL simulators typically account for the impact of small-scale fading effects on the average PHY layer or LL performance, while system level simulations consider large-scale fading contributions (i.e., pathloss and shadowing) to determine the SNR experienced by each transmitted packet and derive the corresponding BLER from the LUTs. In system level simulations, the determined BLER is used to probabilistically estimate whether the received packet is correctly decoded or not. Previous studies have demonstrated that the LUTs accuracy can significantly affect the outcome of system level simulations [4]. Therefore, an accurate system level evaluation of NR V2X SL communications requires BLER versus SNR curves able to precisely capture the PHY layer performance of the system configuration under evaluation. This is a significant challenge for NR V2X SL communications given the large number of configurations stemming from its flexible PHY and medium access control (MAC) layer design. Moreover, the lack of a comprehensive set of BLER versus SNR curves obtained under different settings does not guarantee consistent and comparable results between system level studies that employ LUTs from different sources to evaluate different system configurations.

This study addresses the mentioned limitations by presenting a detailed and standard-compliant LL analysis of NR V2X SL communications that analyzes the impact of important PHY layer aspects, such as the MCS, the transmitter–receiver (Tx–Rx) relative speed, the channel model, and the number of occupied subchannels on the LL performance. The LL analysis has been conducted using a custom MATLAB-based NR V2X SL LL simulator implemented by the authors and openly released at [5], and covers over 1900 system configurations included in the default NR V2X SL parameters set defined by 3GPP and European Telecommunications Standards Institute (ETSI) in [6] and [7]. The default NR V2X SL parameters set identifies a recommended value for the most relevant system settings (e.g., subchannel size, channel bandwidth, SCS), and provides a range of possible values for several MAC and PHY layer configurable parameters. With this study, we also openly release the complete set of standard-compliant NR V2X SL BLER versus SNR curves obtained for all the possible combinations of configurable parameters (1904 in total). To the authors' knowledge, this represents the largest NR V2X SL LL data set openly available, and represents a valuable asset for the community as it provides accurate LL models for thorough NR V2X SL system level investigations under a broad range of settings and configurations. The released BLER versus SNR curves are openly available at [8] in the form of LUTs, and can be easily integrated into any system level or network simulator.

The remainder of this article is organized as follows. Section II reviews existing NR V2X SL LL studies. Section III presents the most relevant PHY layer features of the NR V2X SL standard and Section IV describes the NR V2X SL LL simulator implemented in this study. Section V outlines the fixed and configurable parameters included in the default NR V2X SL parameters set defined by 3GPP and ETSI. Section VI analyzes the impact of relevant PHY layer features and parameters on the LL performance of NR V2X SL communications and, lastly, Section VII draws the conclusions.

II. Related Work

First studies on the LL performance of NR V2X SL communications have been reported in [9], [10], and [11]. Anwar et al. [9] claimed to compare the PHY layer performance of NR V2X SL and IEEE 802.11bd to assess which technology is most suited for the support of eV2X services using vehicle to vehicle (V2V) communications. However, their PHY layer implementation follows 5G NR UL and not NR V2X SL specifications. Similarly, the LL simulator utilized in [10] is based on LTE V2X SL specifications and does not consider relevant PHY layer features of NR V2X SL. As highlighted in [3], the PHY layer of NR V2X SL exhibits remarkable novelties and differences with respect to 5G NR UL/DL and LTE V2X SL. Therefore, the studies in [9] and [10] do not provide an accurate LL evaluation of NR V2X SL communications, and their LL results cannot be used to accurately capture the PHY layer performance of NR V2X SL communications in system level or network simulations. A standard-compliant LL study is reported in [11], where the authors evaluate the design of the new NR V2X SL control channel. However, the LL study reported in [11] does not cover the shared channel that is used to transmit the data payload. The shared channel features a different PHY layer design with respect to the control channel and supports a wider range of MCSs. We should also note that the LL simulators used in [9], [10], and [11] are not openly available. Existing reference open-source 5G NR simulators are the MATLAB-based GTEC 5G [12] and the Vienna 5G LL [13] simulator. The GTEC 5G simulator was developed to evaluate different 5G NR candidate waveforms, while the Vienna 5G LL simulator is a powerful platform that allows an exhaustive evaluation of the 5G NR PHY layer. Yet, both simulators focus on 5G

NR UL and DL communications, and do not implement 5G NR V2X SL communications. More recently, Liu et al. [14] presented an open-source simulator for the LL assessment of 5G NR SL public safety communications. The presented simulator features an accurate 5G NR SL MAC and PHY layer implementation, but it does not implement relevant aspects for the LL evaluation of V2X SL communications, such as the V2V channel models and the MCS tables, defined by 3GPP and included in the default NR V2X SL parameter set (see Section V).

The LL performance of NR V2X SL communications was partially analyzed in several prestandardization 3GPP working groups documents [15], [16], [17], [18], covering a limited set of system configurations. The BLER versus SNR curves reported in [15] have been obtained considering two MCSs (QPSK code rate 0.3 and 64-QAM code rate 0.6) and two different channel models; note that the default NR V2X SL parameters set defined by 3GPP and ETSI includes 28 different MCSs for NR V2X SL and 5 different channel models. The studies in [16] and [17] evaluate the LL performance for the shared and control channel considering a single Tx–Rx relative speed and a single MCS (QPSK code rate 0.5). The study in [18] analyzes the impact of the Tx–Rx relative speed on the NR V2X SL LL performance, but focuses on a single channel model and only two MCSs (QPSK code rate 0.3 and 64-QAM code rate 0.6). Although these studies present valuable insights into the expected LL performance of NR V2X SL communications, we should note that they were not yet based on fully standardized NR V2X SL specifications as they were produced during the standardization process. In addition, they cover only a limited set of parameter settings, and they are not directly comparable since they were conducted using different, and not openly available, LL simulators.

The limited number of NR V2X SL LL studies also impacts the accuracy and scope of system level investigations, as these rely on LL models (e.g., LUTs) to account for PHY layer effects in NR V2X SL system level simulators. To this end, the lack of LL models restricts the number of system configurations that can be accurately analyzed at the system level. Moreover, the comparison of different NR V2X SL system configurations, evaluated using LL models from different sources, may undermine the accuracy of the comparison. As of today, these limitations impact existing NR V2X SL system level or network simulators. For example, the ns-3-based 5G-LENA simulator [19] has been recently extended with a NR V2X SL module [20]. However, the LUTs used in the 5G-LENA NR V2X SL module have been obtained with an LL simulator that follows 5G NR UL/DL specifications [21]. Another open-source NR V2X SL network simulator based on ns-3 was presented by Lusvarghi and Merani [22]. In this case, the LUTs (BLER versus SNR curves) used to represent the control and shared channels PHY layer performance are extracted from the 3GPP working groups documents [16] and [17], respectively. These LUTs adhere to NR V2X SL specifications, but cover a small set of system settings and restrict the number of possible configurations that can be analyzed. The same limitations are encountered in [23], where the authors employ an ns-3-based NR V2X SL network simulator which integrates LUTs from [18] that cover a narrow set of system configurations.

The limited number of NR V2X SL LL studies available in the literature, and the large number of configurable parameters, calls for new LL studies to exhaustively characterize the NR V2X SL LL performance. In this regard, the value of our contribution is twofold. First, we evaluate the impact of relevant PHY layer aspects on the LL performance of NR V2X SL communications using a standard-compliant LL simulator. Second, we openly release the obtained standard-compliant BLER versus SNR curves in the form of LUTs. The released LL data set covers an exhaustive range of system settings defined in the default NR V2X SL parameters set identified by 3GPP and ETSI, thus representing a valuable asset for the community. The data set represents the most comprehensive LL evaluation of NR V2X SL communications reported to date, and it provides a large set of LL models (obtained using the same LL simulator) that can be easily integrated into any system or network level simulator (e.g., the ns-3-based simulators employed in [19], [21], and [22]) to accurately model the PHY layer performance in system level simulations under a wide set of system configurations.

III. NR V2X SL Physical-Layer Structure

A. Organization of Physical Radio Resources

NR V2X SL is characterized by a flexible organization of radio resources in the time and frequency domain. In the time domain, the frame structure consists of 10-ms-long radio frames that are divided into 1-ms subframes. Each subframe includes a variable number of slots depending on the adopted numerology (μ). The number of slots in a subframe is 2^{μ}, and the slot duration is $2^{-\mu}$ ms. NR V2X SL has been designed to operate in the frequency range 1 (410 MHz – 7.125 GHz). In this range, μ can be set to 0, 1, or 2. As a result, each subframe consists of {1, 2, 4} slots of {1, 0.5, 0.25} ms when $\mu = \{0, 1, 2\}$, respectively. A time slot includes 14 OFDM symbols when normal cyclic prefix (CP) is utilized. An extended CP can only be used when μ is equal to 2. In this case, the number of OFDM symbols in a slot is reduced to 12. In the frequency domain, the NR V2X SL radio resources are organized into OFDM subcarriers separated by an SCS equal to $2^{\mu} \times 15$ kHz. NR V2X SL supports SCS values of {15, 30, 60} kHz when $\mu = \{0, 1, 2\}$, respectively.

The resource element (RE) represents the fundamental radio resource unit. An RE consists of a single subcarrier and a single OFDM symbol. Within the same time slot, 12 consecutive OFDM subcarriers form a resource block (RB), and a set of M_{sub} consecutive RBs forms a subchannel. A subchannel is the smallest unit for data transmission and reception in NR V2X SL. M_{sub} defines the subchannel size and it can be equal to 10, 12, 15, 20, 25, 50, 75, or 100 RBs, depending on the channel bandwidth and on the SCS [24].

B. PSSCH and PSCCH

In NR V2X SL, data and control information are transmitted on the physical SL shared channel (PSSCH) and physical SL control channel (PSCCH) [25]. The data information is

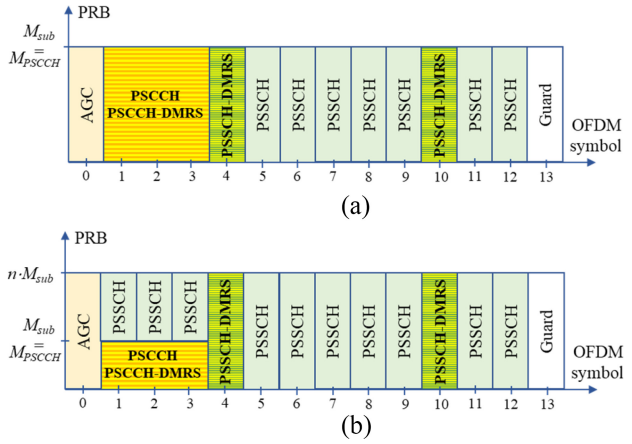

Fig. 1. PSCCH and PSSCH multiplexing in NR V2X SL: Normal CP, three PSCCH OFDM symbols, and two PSSCH-DMRS symbols. (a) 1 subchannel. (b) n subchannels.

organized into transport blocks (TBs) and is transmitted on the PSSCH. Depending on the TB size and on the employed MCS, the PSSCH occupies an integer number n of subchannels. In NR V2X SL, the MCS can be selected from either [26, Table 5.1.3.1-1, Table 5.1.3.1-2, or Table 5.1.3.1-3]. Each TB transmission is associated with its SL control information (SCI). The SCI is transmitted in two stages. The first-stage SCI includes relevant information for the correct decoding of the TB and is transmitted on the PSCCH. The second-stage SCI is transmitted together with the TB on the PSSCH, and it carries information for supporting retransmissions and channel state reports.

In NR V2X SL, the PSSCH and the PSCCH are multiplexed on adjacent and nonoverlapping REs during the same time slot. The multiplexing of PSSCH and PSCCH is a specific feature of NR V2X SL and it is not supported in LTE V2X SL, 5G NR UL, or 5G NR DL. The PSCCH and PSSCH multiplexing is represented in Fig. 1, considering the case in which the PSSCH and the PSCCH occupy the full slot.[1] Fig. 1(a) and (b) illustrate the PSCCH and PSSCH multiplexing when the number of subchannels is equal to 1 and to n ($n > 1$), respectively. Note that, in both figures, the first OFDM symbol within a slot is used for automatic gain control (AGC) purposes, and that the last symbol is used as guard symbol. The AGC symbol is filled with a copy of the second OFDM symbol, whereas the guard symbol is left idle.

1) PSCCH: The PSCCH is mapped to the lowest RBs of the first subchannel utilized for the NR V2X SL transmission [26]. The number M_{PSCCH} of RBs utilized by the PSCCH can be 10, 12, 15, 20, or 25, as long as $M_{\text{PSCCH}} \leq M_{\text{sub}}$. In the time domain, the PSCCH can utilize 2 or three OFDM symbols starting from the second symbol of the slot. Fig. 1 represents the case in which the PSCCH occupies three OFDM symbols. Within the PSCCH, the content of the first-stage SCI follows the SCI format 1-A defined in [25, Sec. 8.3.1]. According to it, the first-stage SCI carries information about the TB priority, the resource reservation period used at the MAC sublayer, the MCS employed to encode the TB and the second-stage SCI format among others. The size of the first-stage SCI ranges from 20 to 43 bits depending on the configuration of higher layer parameters.

2) PSSCH: The PSSCH accommodates the transmission of both the second-stage SCI and the TB. This is a distinctive feature of NR V2X SL with respect to 5G NR UL and DL, where data and control information are transmitted on separate channels. The second-stage SCI can be formatted according to the SCI format 2-A (35 bits long) or 2-B (48 bits long) defined in [25, Sec. 8.4.1] (Section VIII-D1). Both formats include information related to hybrid automatic repeat request (HARQ) retransmissions and a cast type indicator that allows to discriminate between unicast, groupcast, and broadcast communications. The second-stage SCI is also used to transmit channel state reports. The TB and the second-stage SCI are separately encoded and multiplexed into a single codeword prior to OFDM modulation. The multiplexing operation depends on the number of multiple input multiple output (MIMO) transmission layers [25]. The number of MIMO layers is limited to 2 in NR V2X SL.

C. DMRS Patterns

DMRSs are used by the receiver to estimate the radio channel response and guarantee proper demodulation of the received signals. NR V2X SL defines dedicated DMRS patterns for the PSSCH and the PSCCH. The number of symbols used to accommodate the PSSCH-DMRSs can be equal to 2, 3 or 4 symbols. The position of the PSSCH-DMRS symbols within a slot depends on the duration of the PSCCH (i.e., two or three symbols) and on the total number of slot symbols. For example, the PSSCH-DMRS symbols are located at symbols 4 and 10 in Fig. 1. If three symbols were utilized for the PSSCH-DMRS, they would have been located at symbols 1, 6, and 11 in Fig. 1. If four symbols were utilized for the PSSCH-DMRS, they would have been located at symbols 1, 4, 7, and 10. A complete list of the allowed PSSCH-DMRS configurations is available in [27, Table 8.4.1.1.2-1]. It should be noted that PSSCH-DMRS configurations that utilize more than two symbols multiplex the first PSSCH-DMRS symbol (located at symbol 1) with the PSCCH on frequency-adjacent REs. When a NR V2X SL transmission utilizes a single subchannel, the multiplexing of PSSCH-DMRS and PSCCH on symbol 1 is only supported if $M_{sub} \geq 20$ RBs, as explained in [26, Sec. VIII-B2]. If $M_{sub} < 20$ RBs, the first subchannel only supports the configuration with two PSSCH-DMRS symbols. It is also important to note that PSSCH-DMRSs occupy one every two REs within the allocated OFDM symbols, as explained in [27, Sec. VIII-D1.II-B]. The REs that are not utilized for PSSCH-DMRS signals are utilized to accommodate the PSSCH.

The DMRS signals associated to the PSCCH occupy one every four REs in the symbols allocated for the PSCCH and PSCCH-DMRS transmission (see [27, Sec. VIII-D1.III-B]). The PSCCH is transmitted in the REs that are not utilized to accommodate PSCCH-DMRS.

IV. NR V2X SL Link Level Simulator

This section describes the NR V2X SL LL simulator developed to evaluate the LL performance of NR V2X SL

[1] NR V2X SL also supports configurations in which the PSSCH and PSCCH occupy from seven to 14 OFDM symbols within a slot [25].

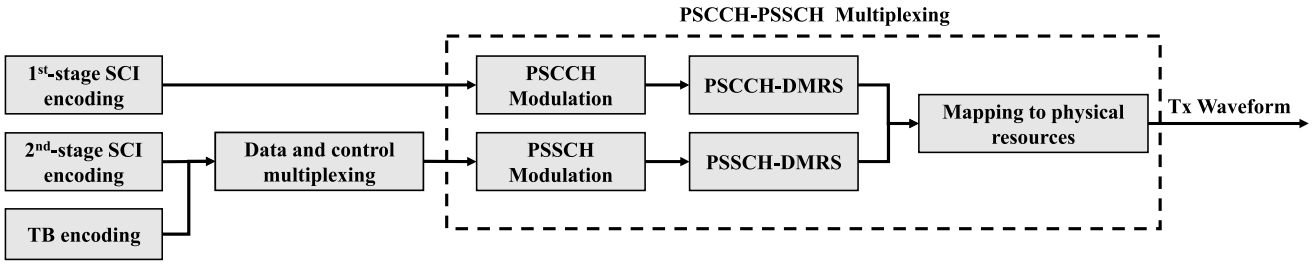

Fig. 2. Transmitter chain.

communications and obtain the BLER versus SNR curves presented and openly released in this work. The simulator is implemented in MATLAB using the 5G Toolbox functionalities (version R2022a), and adheres to the NR V2X SL specifications published in Release 16 [28]. As the 5G toolbox provides standard-compliant functions for 5G NR UL and DL only (and not NR V2X SL), significant efforts were devoted to the implementation of the new NR V2X SL PHY layer features, namely, the following: 1) implementation of the first-stage and second-stage SCIs introduced in NR V2X SL; 2) development of a new set of functions to determine the TB size and properly format the first-stage and second-stage SCI; 3) customization of the encoding, decoding, modulation, and demodulation functionalities according to NR V2X SL specifications; 4) implementation of the new PSCCH and PSSCH multiplexing mechanism defined in NR V2X SL; 5) implementation of the new NR V2X SL PSCCH-DMRS and PSSCH-DMRS patterns; and 6) implementation of a new set of NR V2X SL channel models that adheres to the 3GPP evaluation guidelines [6].

The three main building blocks of the LL simulator are the transmitter chain (Section IV-A), the channel model (Section IV-B), and the receiver chain (Section IV-C). TBs and their associated SCIs are generated and processed by the transmitter chain, passed through the channel model, and decoded by the receiver chain.

A. Transmitter Chain

Fig. 2 outlines the different modules included within the transmitter chain of the NR V2X SL LL simulator. The transmitter chain is responsible for the encoding, modulation, and transmission of the generated data. Differently from its 5G NR UL and DL counterparts, NR V2X SL multiplexes the transmission of PSCCH and PSSCH on the same RBs, as discussed in Section III. Therefore, the transmitter chain of our NR V2X SL LL simulator features a more complex structure with respect to existing 5G NR UL/DL LL simulators [12], [13], [21].

1) First-Stage SCI Encoding: The first operation of the transmitter chain consists in the encoding of the first-stage SCI. The "First-Stage SCI Encoding" module implements a custom function that formats the content of the first-stage SCI following the SCI format 1-A definition reported in Section III. Following NR V2X SL specifications ([25, Sec. 8.3.2-8.3.4]), the first-stage SCI encoding block performs the following sequence of operations on the content of the first-stage SCI: 24-bit cyclic redundancy check (CRC) attachment, polar encoding, and polar code rate matching [25]. These operations are inherited from NR DL specifications, although there are some differences. During the CRC attachment phase, the payload of the first-stage SCI is used to compute 24 parity bits. Differently from NR DL, the first-stage SCI codeword (payload plus CRC) is not scrambled after the CRC attachment. The amount of redundancy introduced during the encoding process depends on the number of REs available within the PSCCH (excluding the PSCCH-DMRS REs).

2) Second-Stage SCI Encoding: The "Second-Stage SCI Encoding" module includes custom functions that allow the formatting of the second-stage SCI according to either the SCI format 2-A or the SCI format 2-B reported in Section III. Regardless of the format, the second-stage SCI bits undergo the same sequence of CRC attachment, Polar coding and rate matching operations employed for the first-stage SCI, although with some minor modifications [25]. The target code rate of the second-stage SCI is determined as a function of several parameters, namely, the associated TB code rate, the size of the selected second-stage SCI format, and the number of subcarriers occupied by the PSSCH. Our NR V2X SL LL simulator implements the formatting of the second-stage SCI and the calculation of its target code rate.

3) TB Encoding: The implementation of the "TB encoding" module has required custom functions that are not available within MATLAB's 5G Toolbox. These functions are responsible for generating and encoding the TB information bits. First, the TB size is determined following the two-step process defined in [26, Sec. 8.1.3.2]. The TB size depends on the length of the rate matched second-stage SCI, the PSSCH-DMRS pattern, the number of PSCCH REs, the selected MCS index, and the number of available REs in the PSSCH. Next, TB encoding is performed based on the following sequence of operations: 24-bit CRC attachment, low-density parity-check (LDPC) encoding, and rate matching (see [25, Sec. 8.2]).

4) Data and Control Multiplexing: The "Data and control multiplexing" module is responsible for multiplexing the output of the second-stage SCI encoding and TB encoding blocks into a single codeword. This is a specific feature of NR V2X SL that we implemented in our simulator. The data and control multiplexing operations depend on the number of MIMO transmission layers ([25, Sec. 8.2.1]). When only 1 transmission layer is considered, the second-stage SCI and TB bits are concatenated.

5) PSCCH-PSSCH Multiplexing: In the "PSCCH-PSSCH Multiplexing" module, the control channel and the shared channel codewords are modulated and allocated on the NR time-frequency grid together with their associated DMRS symbols. The control channel codeword is provided by the first-stage SCI encoding block and is accommodated over the PSCCH. The shared channel codeword is generated by the data and control multiplexing module and is allocated over the PSSCH. As shown in Fig. 2, the PSCCH and the PSSCH are processed independently until they are mapped on physical resources. The operation of each block is summarized next:

PSCCH Modulation: Prior to modulation, the bits of the first-stage SCI codeword undergo a scrambling operation. Scrambling is implemented by means of an XOR operation between the codeword and a pseudo-random scrambling sequence, as in 5G NR UL/DL. In our NR V2X SL implementation, the pseudo-random sequence of bits is initialized with a fixed value following the specifications in [27, Sec. 8.3.2.1] and is seeded with different values for each transmission. Then, the block of scrambled bits is QPSK-modulated to generate the PSCCH OFDM symbols.

PSCCH-DMRS: This module exploits a new function to generate the DMRS symbols associated with the PSCCH. The generation of the PSCCH-DMRS symbols follows the SL specifications in [27]. Accordingly, the PSCCH-DMRS symbols are generated using a pseudo-random sequence whose initialization value is set by the scramble ID provided by higher layers. In our implementation, we set the scramble ID to 0.

PSSCH Modulation: In the "PSCCH modulation" module, the second-stage SCI and TB bits are separately scrambled employing two different pseudo-random scrambling sequences. Each scrambling sequence is initialized using the decimal representation of the CRC associated with the first-stage SCI and is seeded with different values for each transmission. Then, the scrambled bits of the second-stage SCI are modulated using QPSK modulation, whereas the modulation order of the TB bits depends on the selected MCS. After modulation, the PSSCH OFDM symbols undergo a layer mapping and a noncodebook-based precoding procedure before being allocated on the corresponding resources.

PSSCH-DMRS: The "PSSCH-DMRS" module has been implemented to allow all the DMRS time pattern configurations reported in SL specifications (see [27, Table 8.4.1.1.2-1]). A new function has been developed to generate the DMRS symbols associated with the PSSCH. In NR V2X SL, the generation of the PSSCH-DMRS symbols is based on a pseudo-random sequence which is initialized using the decimal representation of the first-stage SCI CRC.

Mapping to Physical Resources: This module performs the last operation of the PSSCH-PSCCH multiplexing block, and is responsible for the allocation of the PSSCH, PSCCH, PSSCH-DMRS and PSCCH-DMRS OFDM symbols on the corresponding REs within the NR V2X SL time-frequency grid. To do so, we have developed a new function that implements the time-frequency organization of radio resources illustrated in Section III. In our implementation, the NR V2X SL time-frequency grid is represented as a matrix where each element corresponds to a distinct RE. The "Mapping to physical resources" block assigns the RE indexes to the different components. AGC and guard symbols are also included (see Fig. 1). Once the PSSCH and PSCCH have been mapped to their respective REs along with the associated DMRS symbols, the time-frequency resource grid is converted into a time-domain CP-OFDM waveform using MATLAB's built-in UL/DL functions. The transmission of the CP-OFDM waveform is the last step of the transmitter chain.

B. Channel Model

To capture the small-scale fading effects which impair NR V2X SL communications, we have implemented in our LL simulator the V2V clustered delay line (CDL) channel models defined by 3GPP in its evaluation guidelines [6]. A CDL channel represents the received signal as the superposition of different clusters of echoes. Each cluster is defined with a specific delay, attenuation, arrival, and departure angle. The V2V CDL channel models encompass SL communications occurring in two propagation environments, namely, Highway and Urban. For each environment, two different CDL models are defined based on the V2V link state.

1) *Line of Sight (LOS):* The Tx–Rx link is characterized by a direct LOS path.
2) *NLOSv:* The LOS path is blocked by the presence of other vehicles.

In the urban setting, an additional channel state is considered.

1) *NLOS:* The LOS path is blocked by the presence of buildings.

In our NR V2X SL LL simulator, each channel model is implemented with a custom configuration of MATLAB's built-in CDL system object originally defined for 5G NR UL/DL simulations. The configuration of the CDL channels in the NR V2X SL LL simulator follows the models reported in [6, Tables 6.2.3.1-1–6.2.3.1-5]. In addition, each CDL channel model can be customized with specific maximum Doppler shift and Tx–Rx antenna array configurations. The maximum Doppler shift property allows to model different relative speed values between the transmitting and receiving vehicles. The Tx–Rx antenna array property allows the configuration of the number of radiating elements and their radiation pattern. With respect to 5G NR UL/DL simulations, the CDL channel models implemented in our simulator feature a horizontal, rather than vertical, MIMO arrangement of isotropic (or V2X-specific) antenna models following the 3GPP guidelines in [6]. Our channel model implementation also features an additive white Gaussian noise (AWGN) contribution whose variance depends on the examined SNR value.

C. Receiver Chain

The receiver chain processes the channel-impaired CP-OFDM waveform that is captured by each of the receiving antennas following the sequence of operations described in Fig. 3. Fig. 3 shows that the recovery of the PSSCH and PSCCH information is carried out on two different receiver chain branches. This is the case because the PSCCH and the

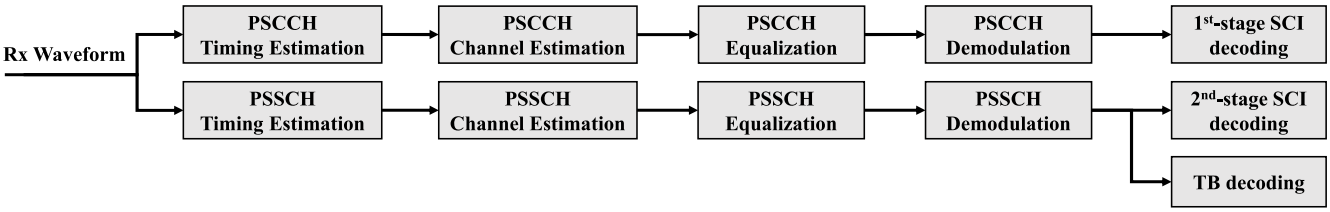

Fig. 3. Receiver chain.

PSSCH employ distinct DMRS symbols and undergo separate channel estimation and equalization operations. This is another relevant difference with respect to LTE V2X SL and existing 5G NR UL/DL simulators, and it required significant implementation efforts. For both PSSCH and PSCCH, the DMRS symbols are used to perform timing and channel estimation. After having estimated the channel response, equalization is used to reconstruct the originally transmitted PSSCH and PSCCH symbols constellations. Specifically, the NR V2X SL LL simulator employs minimum mean square error (MMSE) equalization.

After the equalization step, demodulation and first-stage SCI decoding are the next operations within the receiver chain if we concentrate on the PSCCH branch. The "PSCCH demodulation" and first-stage SCI decoding modules perform the inverse operations with respect to their transmitter chain counterparts, i.e., the PSCCH modulation and first-stage SCI encoding modules reported in Fig. 2. Specifically, the Polar decoding process uses a CRC-aided successive-cancelation list decoder of length L. In our implementation, we set L to its maximum allowed value (i.e., $L = 8$) as it guarantees the best error correction performance [29].

On the PSSCH branch, the PSSCH demodulation, second-stage SCI decoding, and "TB decoding" modules follow the PSSCH equalization step. The PSSCH demodulation module includes a custom piece of code that separates the second-stage SCI and TB symbols. This is done to guarantee a proper demodulation process since the second-stage SCI and TB symbols might employ different modulation orders. We should recall that the TB modulation depends on the selected MCS, whereas the second-stage SCI always utilizes QPSK modulation. After the demodulation step, the second-stage SCI and TB bits undergo their corresponding decoding operations. The second-stage SCI employs the same Polar decoder configuration used for the first-stage SCI. In the TB case, LDPC decoding is carried out using the "Normalized min-sum" algorithm and by setting the maximum number of LDPC decoding iterations to 6, i.e., following the default settings employed by MATLAB's 5G toolbox in 5G NR UL simulations. Both the PSSCH and the PSCCH receiver branch are based on soft-decision decoding techniques.

V. NR V2X SL Parameters Set

NR V2X SL communications are characterized by a large number of configurable parameters and most of the studies reported to date use different configurations, thus hindering the definition of a common evaluation framework for the assessment of the NR V2X SL performance. To address this challenge, 3GPP and ETSI working groups have introduced default NR V2X SL methodologies and parameter settings in [6] and [7]. The introduction of a default NR V2X SL parameters set facilitates a more fair and accurate comparison of the performance of NR V2X SL communications. A default parameters set is also particularly useful when direct V2V communications are considered, as it allows vehicles to leverage a common system setting and exchange information without the intervention of the cellular infrastructure.

3GPP has defined a common evaluation methodology for the analysis of NR V2X SL communications in [6], covering a wide range of LL and system level assumptions. For example, 3GPP indicates the NR V2X SL operating frequency, the number of transmitting and receiving antennas, the antenna radiating pattern, and the vehicles' speed in highway and urban environments. However, the 3GPP evaluation methodology does not provide any indication regarding the configuration of the numerous NR V2X SL MAC and PHY layer parameters. Therefore, we have complemented the information in [6] with the recommended access layer configuration identified by ETSI in [7] to define a default NR V2X SL set of parameters. In [7], ETSI indicates a default configuration for all the radio resource control (RRC), radio link control (RLC), MAC, and PHY layer parameters employed in NR V2X SL communications. As an example, [7] includes the recommended channel bandwidth, SCS, subchannel size, and MCS table.

Table I summarizes the parameter settings included in the default NR V2X SL parameters set defined following [6] and [7]. The table includes fixed parameters that are not changed across simulations, and configurable parameters that we vary across simulations to analyze their impact on the LL performance of NR V2X SL communications. We have evaluated all possible combinations of configurable parameters (1904 in total), and we openly release with this article the complete set of BLER versus SNR curves at [8]. For example, the Highway LOS channel model includes 28 MCSs, 4 relative speed settings, and 4 different subchannels configurations. This corresponds to a total of $28 \cdot 4 \cdot 4 = 448$ BLER curves only for the Highway LOS case. Table I(a) and (b) report the default NR V2X SL parameters set provided by 3GPP in [6]. According to Table I(a), we considered NR V2X SL radios operating at 5.9 GHz with 2 Tx and 4 Rx isotropic antennas in all simulations. The number of MIMO transmission layers is set to one. We evaluate the LL performance and derive BLER curves for all the channel models reported in Table I(b): Highway LOS and NLOSv, and Urban LOS, NLOSv, and

TABLE I
DEFAULT NR V2X SL PARAMETERS SET. (A) FIXED PARAMETERS FROM 3GPP [6]. (B) CONFIGURABLE PARAMETERS FROM 3GPP [6]. (C) FIXED PARAMETERS FROM ETSI [7]. (D) CONFIGURABLE PARAMETERS FROM ETSI [7]

(a)

Parameter	Value
Operating Frequency	5.9 GHz
Number of Tx-Rx antennas	2 Tx 4 Rx
Antenna type	Isotropic
Number of Tx layers	1

(b)

Parameter	Value
Channel models, Highway	{LOS, NLOSv}
Channel models, Urban	{LOS, NLOS, NLOSv}
v_{rel}, Highway	{0, 70, 140, 280} km/h
v_{rel}, Urban	{0, 60, 120} km/h

(c)

Parameter	Value
Bandwidth	20 MHz
Subcarrier spacing	30 kHz
OFDM symbols per slot	14
Subchannel size	12 RBs
Available subchannels	4
PSCCH RBs	12 RBs
PSCCH OFDM symbols	3
PSSCH-DMRS Pattern	{2}

(d)

Parameter	Value
MCS	28 possible MCSs from Table 5.1.3.1-2 [26]
Number of subchannels N_{sub}	{1, 2, 3, 4}

NLOS. Another relevant simulation parameter is the vehicles' speed, since the relative speed between vehicles (v_{rel}) affects the maximum Doppler shift experienced by a V2V link. Following [6], the vehicles' speed in the highway environment can be either set to 70 or 140 km/h, which results in relative speeds between vehicles of: 0, 70, 140, or 280 km/h. In the urban environment, the vehicles' speed is fixed to 60 km/h, and therefore the v_{rel} values are limited to 0, 60 and 120 km/h.

The settings of the default NR V2X SL parameters set defined by ETSI [7] are reported in Table I(c) and (d). All simulations consider a 20 MHz wide channel, a 30 kHz SCS and 14 OFDM symbols per slot. According to [24], the total number of available RBs in each slot is equal to 51. Since the subchannel size is 12 RBs [7], the total number of available subchannels in a single slot is 4. Accordingly, the number of employed subchannels, N_{sub}, is configurable and can vary from 1 to 4. The PSCCH is 12 RBs long and occupies three consecutive OFDM symbols. With NR V2X SL, vehicles can either use 2, 3 or four PSSCH-DMRS symbols in the same slot. However, only the two PSSCH-DMRS option is allowed in the $N_{\text{sub}} = 1$ case when the subchannel size is smaller than 20 RBs (see Section III). For this reason, we decided to employ the two PSSCH-DMRS pattern (indicated as {2} by the standard in [26]) in all our LL simulations. The MCS can be selected from [26, Table 5.1.3.1-2] that includes a total of 28 different MCSs [Table I(d)]. The MCS choices range from QPSK modulation with a 120/1024 target code rate (indicated as QPSK-120) to QPSK-602, from 16QAM-378 to 16QAM-658, from 64QAM-466 to 64QAM-873, and from 256QAM-682.5 to 256QAM-948.

VI. NR V2X SL LINK LEVEL PERFORMANCE

This section analyzes the impact of key PHY layer aspects, such as the Tx–Rx relative speed, the communication channel, and the MCS on the NR V2X SL LL performance. The LL performance is represented with BLER versus SNR curves obtained varying the average SNR and measuring the BLER per average SNR value; the SNR range is a configurable parameter of our simulator. The BLER is computed as the fraction of incorrectly received transmissions with respect to the total number of transmissions. For each average SNR value, we simulated 1×10^4 TB plus SCI transmissions, which is deemed a sufficiently high number of channel realizations to guarantee the statistical accuracy of the presented results. The relative MOE_{95}, i.e., the relative margin of error measured for a 95% confidence interval, is below 0.007 for all the obtained results. Due to space constraints, this section only reports the LL performance for a confined set of parameters. However, the full set of BLER versus SNR curves, obtained for all 1904 possible combinations of parameters in Table I is openly available at [8]. This provides the community with a comprehensive data set of standard-compliant LL performance results that, in addition, can be easily integrated into any system level or network simulator for an accurate and exhaustive system level evaluation of NR V2X SL communications.

Unless otherwise stated, the results reported in this section consider the Highway LOS channel model, $v_{\text{rel}} = 0$ km/h, $N_{\text{sub}} = 1$ and four different MCSs: 1) QPSK-308; 2) 16QAM-490; 3) 64QAM-616; and 4) 256QAM-797.

A. Decoding of First-Stage SCI, Second-Stage SCI, and TB

NR V2X SL transmissions include a TB and its associated first-stage and second-stage SCIs. TB, first-stage SCI, and second-stage SCI are transmitted on different REs and undergo dedicated encoding and modulation mechanisms (see Section IV). Therefore, their PHY layer performance is different, and the implemented LL simulator is able to separately evaluate the first-stage SCI, second-stage SCI, and TB PHY layer performance, deriving dedicated BLER versus SNR curves for each component. We should note that none of the existing NR V2X SL LL studies separately analyzes the first-stage SCI, second-stage SCI, and TB LL performance.

Fig. 4 reports the first-stage SCI, second-stage SCI, and TB BLER curves obtained when the TB transmission employs different MCSs. This figure shows that the transmission of the first-stage SCI is the most robust one as it experiences the best BLER performance. As a matter of fact, the first-stage SCI employs the most robust MCS (i.e., QPSK-84). The MCS of the first-stage SCI is fixed and it is not affected by the MCS used for transmitting the TB. In addition, also the first-stage SCI length and the size of the PSCCH do not depend on the MCS of the TB. As a result, the first-stage

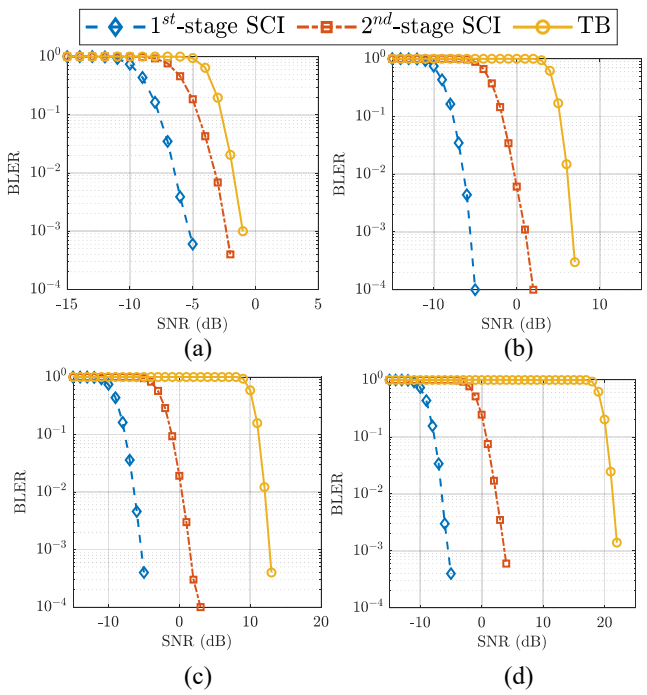

Fig. 4. First-stage SCI, second-stage SCI, and TB: BLER versus SNR curves for different TB MCSs. (a) QPSK-308. (b) 16QAM-490. (c) 64QAM-616. (d) 256QAM-797.

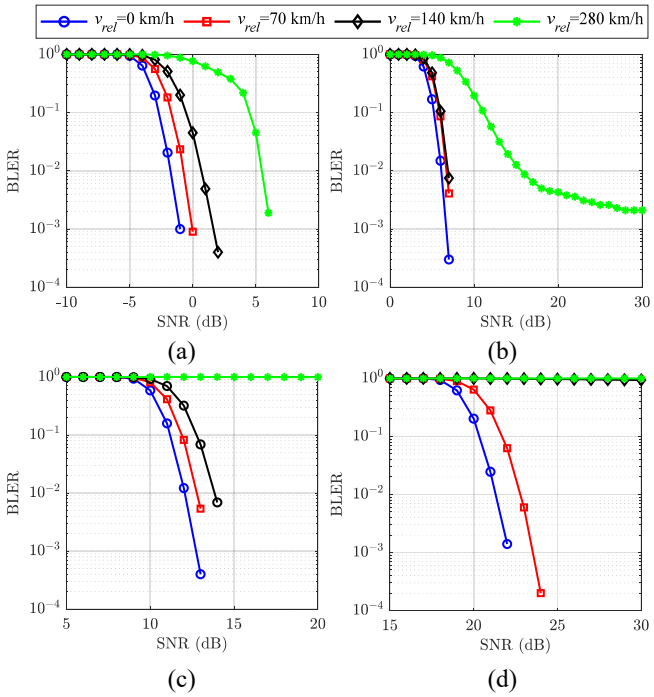

Fig. 5. Impact of the Tx–Rx relative speed on the TB BLER for different TB MCSs. (a) QPSK-308. (b) 16QAM-490. (c) 64QAM-616. (d) 256QAM-797.

SCI BLER curve is identical from Fig. 4(a)–(d). Conversely, the code rate of the second-stage SCI depends on the MCS of the associated TB (see Section IV-A). In detail, the code rate of the second-stage SCI is 272/1024, 432/1024, 539/1024, and 703/1024 from Fig. 4(a)–(d), respectively. The second-stage SCI is always transmitted using QPSK modulation. The code rate of the second-stage SCI is always larger than the one employed by the first-stage SCI, thus resulting in a less robust transmission as highlighted by Fig. 4(a)–(d). With respect to the associated TB, Fig. 4 shows that the second-stage SCI is always characterized by a better PHY layer performance. In Fig. 4(a), the second-stage SCI and the TB employ the same modulation scheme (i.e., QPSK), but the second-stage SCI features a more robust (smaller) code rate. In Fig. 4(b)–(d), the second-stage SCI is always transmitted using QPSK modulation, whereas the TB employs less robust modulation schemes that result in a worse BLER performance.

The difference between the TB and the first-stage SCI BLER performance increases as we use a less robust but more spectrally efficient MCS for the transmission of the TB [from Fig. 4(a)–(d)]. This is the case since, as the spectral efficiency of the MCS increases, each TB can accommodate a larger number of information bits, but its BLER performance significantly deteriorates. Fig. 4 shows that the first-stage SCI BLER is almost equal to zero for SNR values larger than -5 dB, and that the content of the first-stage SCI can be correctly recovered also when the decoding of the associated TB fails. In NR-V2X SL communications, vehicles employ the first-stage SCI to reserve transmission resources. Its correct decoding is therefore important to guarantee that other vehicles are aware of the resources utilized by the transmitting vehicle and potentially avoid packet collisions.

The results reported in Fig. 4 clearly show the differences in LL performance for the first-stage SCI, second-stage SCI, and TB. These differences highlight the need to use distinct BLER versus SNR curves to separately evaluate the first-stage SCI, second-stage SCI, and TB decoding probability in system level evaluations.

B. Tx–Rx Relative Speed

Vehicles may have different traveling speed and directions. Depending on the speed and traveling direction of the transmitting and receiving vehicles, a V2V link can experience different relative speeds. At the PHY layer, variations in the relative speed affect the maximum Doppler shift that impairs the transmitted waveform. Doppler shifts can significantly deteriorate the BLER performance depending on the (PSSCH/PSCCH)-DMRS pattern and the employed MCS. In this regard, an accurate LL analysis of NR V2X SL is instrumental to accurately capture the impact of the Tx–Rx relative speed on the BLER versus SNR performance. In the remainder of this section, we separately analyze the BLER performance of the TB and of the first and second-stage SCIs considering different Tx–Rx relative speed values.

1) TB: Fig. 5 reports the BLER performance attained by the TB transmission considering different MCSs and the four relative speed values identified by 3GPP for the highway environment, i.e., $v_{\text{rel}} = \{0, 70, 140, 280\}$ km/h. Note that the SNR ranges reported in Figs. 4 and 5 are different although the considered MCS configurations are the same. Fig. 5(a) quantifies the impact of the relative speed on the TB BLER versus SNR curves in the QPSK-308 case. Despite being a robust MCS choice, the BLER performance deteriorates as the relative speed increases. The employed PSSCH-DMRS pattern

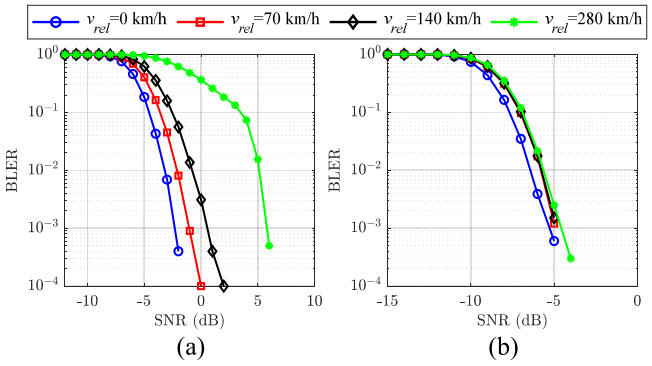

Fig. 6. Impact of the Tx–Rx relative speed on the second-stage SCI and first-stage SCI BLER. (a) Second-stage SCI. (b) First-stage SCI.

is not able to effectively combat the Doppler shift impairments which affect the quality of V2V links. For example, the SNR corresponding to BLER $= 0.01$ increases from -1.8 dB to 5.5 dB when the relative speed augments from $v_{\text{rel}} = 0$ km/h to $v_{\text{rel}} = 280$ km/h. Such 7.3 dB difference can have a significant impact on the quality of V2V communications at the link and system levels and, therefore, on the V2V communication range. With less robust MCSs, the impact of the Doppler shift on the TB PHY layer performance is more evident. In Fig. 5(b), the BLER achieved by a TB transmitted using the 16QAM-490 MCS settles at 0.002 when $v_{\text{rel}} = 280$ km/h and the SNR is higher than 25 dB. The presence of an error floor means that the correct decoding of the received packets cannot be guaranteed for any SNR value. The negative impact of the Tx–Rx relative speed on the PHY layer performance is further highlighted in Fig. 5(c) and (d), where the LL performance of TB transmissions is analyzed considering the 64QAM-616 and 256QAM-797 MCSs, respectively. In Fig. 5(c), the received packet can be correctly decoded only if v_{rel} is equal or smaller than 140 km/h. When $v_{\text{rel}} = 280$ km/h, the considered PSSCH-DMRS pattern is not sufficiently robust to compensate for the Doppler shift and the BLER is equal to 1. In this case, it is not possible to correctly receive any packet, regardless of the SNR value. When the least robust 256QAM-797 MCS is considered, Fig. 5(d) shows that the BLER is equal to 1 starting from relative speeds greater or equal than 140 km/h. The impact of the Tx–Rx relative speed on the TB PHY layer performance illustrated in Fig. 5 has been observed also for other NR V2X SL configurations (see Table I).

2) First-Stage and Second-Stage SCI: Next, we analyze the impact of the relative speed on the second-stage and first-stage SCI in Fig. 6(a) and (b), respectively. The second-stage SCI is multiplexed on the PSSCH together with the associated TB and its decoding process leverages the same PSSCH-DMRS pattern considered in the TB analysis. Since the second-stage SCI always employs QPSK modulation, the impact of the relative speed on its LL performance is similar to the one reported in Fig. 5(a), where the TB BLER was analyzed considering the same modulation scheme. The first-stage SCI is also transmitted using QPSK modulation, but it is encoded with a high-redundancy code rate (see Section VI-A). In addition, the first-stage SCI is transmitted on the PSCCH and

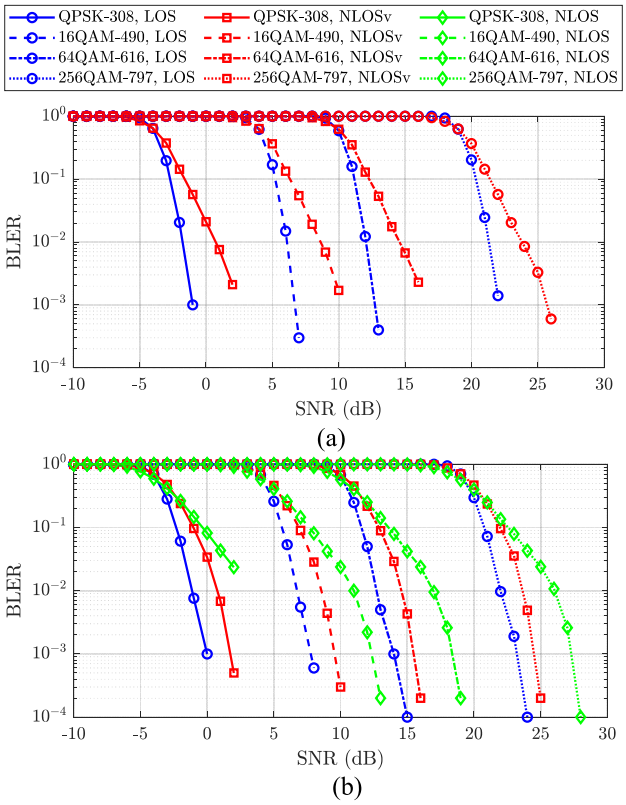

Fig. 7. TB BLER as a function of the SNR for different channel models and states. (a) Highway. (b) Urban.

employs a more robust PSCCH-DMRS pattern with respect to its PSSCH counterpart. As a result, the transmission of the first-stage SCI is extremely robust and can withstand large relative speed values without suffering any degradation in the BLER performance. This is visible in Fig. 6(b), where the first-stage SCI BLER does not significantly change when increasing the relative speed.

This section showed that the first-stage SCI can be correctly decoded under large Tx–Rx relative speeds, even when the associated TB and the second-stage SCI decoding fail due to error floors in the BLER performance. As mentioned in Section VI-A, the correct decoding of the first-stage SCI is crucial for an efficient management of the radio resources and to minimize the risk of packet collisions in NR V2X SL communications.

C. Channel Models

The results presented so far have been obtained considering the Highway LOS channel model. 3GPP guidelines define five different CDL channel models for the evaluation of NR-V2X SL communications, namely, Highway LOS and NLOSv, and Urban LOS, NLOSv, and NLOS. Each channel model is characterized by specific fast-fading parameters, and the results reported in this section highlight the impact of these parameters on the NR V2X SL LL performance.

Fig. 7(a) illustrates the impact of LOS and NLOSv conditions on the TB BLER performance in the highway scenario for different MCSs. As expected, the NLOSv condition

results in a worse BLER performance with respect to its LOS counterpart. For example, the difference between LOS and NLOSv curves is 2.6 dB when the BLER = 0.01 and QPSK-308 MCS is examined in Fig(a). Similar trends can be observed in Fig. 7(a) also for 16QAM-490, 64QAM-616, and 256QAM-797 MCSs.

Fig. 7(b) reports the BLER experienced by the TB transmission in the urban environment, considering LOS, NLOSv, and NLOS propagation conditions. Like in Fig. 7(a), the Urban NLOSv channel results in a worse BLER performance with respect to its Urban LOS counterpart. In the urban environment, NLOS propagation conditions consider the presence of buildings and further degrade the BLER. In the 16QAM-490 case, the SNR difference for a BLER = 0.01 grows from 2 dB to 4 dB when comparing LOS curves with their NLOSv and NLOS counterparts, respectively.

The impact of LOS, NLOSv, and NLOS conditions on the BLER performance illustrated in Fig. 7(a) and (b) has been observed for all the MCSs included in the default NR V2X SL parameters set (see Section V). It is therefore important to employ dedicated BLER versus SNR curves for each channel model when modeling the PHY layer performance at the system level under different propagation conditions.

D. MCS Selection

3GPP NR-V2X SL specifications do not provide any indication regarding the MCS selection, which is left to each specific implementation [30]. Vehicles are allowed to change the employed MCS on a TB-basis. For example, a vehicle might use a more spectrally efficient MCS when the size of a TB augments so that it can fit a larger amount of information in the same number of subchannels. However, the MCS cannot be naively changed without properly modeling its implications at PHY layer, since each MCS is characterized by different robustness levels against channel impairments. This section quantifies the impact of the MCS selection on the TB BLER performance. The MCS employed by the TB does not affect the first-stage SCI PHY layer performance, since the first-stage SCI employs a fixed MCS. The MCS used for the TB transmission has little impact on the second-stage SCI BLER too, since it conditions the code rate of the second-stage SCI but it does not affect its modulation, which is fixed to QPSK.

Fig. 8 reports the TB BLER as a function of the SNR, considering a representative set of MCSs from the default NR V2X SL parameters set (see Table I and Section V). Due to space constraints, we could not report the performance for all the MCSs included in the default set of parameters. However, the BLER versus SNR curves obtained for all MCSs are openly available at [8].

For each modulation scheme, Fig. 8 reports the BLER curves that correspond to the smallest and the largest code rates. As a result, this figure allows to identify the interval of SNR values within which all the BLER curves corresponding to a given modulation scheme lie. Fig. 8 sheds light on the BLER degradation associated with the selection of a more spectrally efficient (i.e., less robust) MCS. For example, a TB

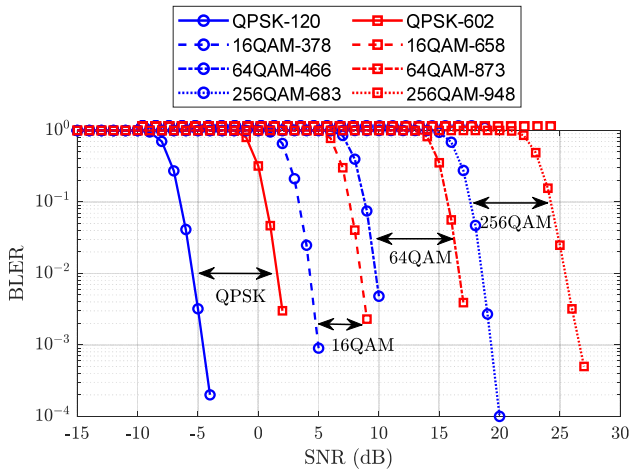

Fig. 8. Impact of the MCS on the TB BLER performance as a function of the SNR.

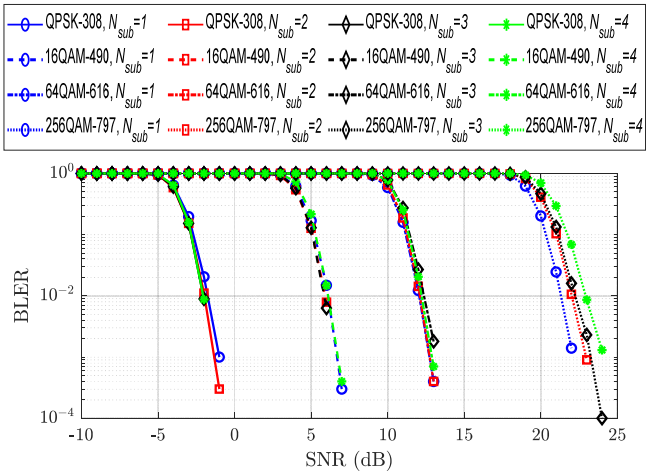

Fig. 9. Impact of N_{sub} on the TB BLER performance.

transmitted using 16QAM-658 requires an approximately 7 dB larger SNR to get the same BLER = 0.01 performance compared to a TB transmitted with QPSK-602 MCS. This effect has important implications on the NR V2X SL performance attained by different MCSs that cannot be neglected when, for example, designing adaptive MCS algorithms. The sound design and the evaluation of such algorithms at the system level must be performed employing LL models that accurately quantify the impact of the MCS selection on the BLER performance.

E. Number of Subchannels

When the MCS is fixed, the number of subchannels required for the transmission of a TB depends on the size of the generated TB. This section analyzes the impact that a variable number of subchannels has on the LL performance of the TB.

Fig. 9 reports the BLER curves obtained when the number of occupied subchannels ranges from 1 to 4, namely, $N_{\text{sub}} = \{1, 2, 3, 4\}$. Fig. 9 shows that the number of occupied subchannels does not affect the TB BLER performance when using QPSK-308, 16QAM-490, and 64QAM-616 MCSs. In

this case, increasing the number of occupied subchannels does not have any impact on the correct decoding of the packet at the PHY layer. On the other hand, Fig. 9 shows that, with 256QAM-797, the BLER performance deteriorates as N_{sub} increases from 1 to 4. For example, a TB transmitted over $N_{\text{sub}} = 4$ subchannels requires a 2 dB larger SNR to achieve a BLER of 0.01 with respect to the $N_{\text{sub}} = 1$ setting. The impact of N_{sub} on the TB BLER is the same also for the other MCSs included in the default NR V2X SL parameters set and not reported in Fig. 9. These results indicate that N_{sub} can have an impact on the LL performance, and dedicated BLER curves are necessary to properly model the impact of N_{sub} at PHY layer, especially when considering high-order modulation schemes (e.g., 256 QAM).

VII. Discussion and Conclusion

This work has analyzed the LL performance of NR V2X SL communications, a fundamental technology for the realization of the IoV paradigm. The study has been conducted using a MATLAB-based LL simulator implemented by the authors following 3GPP specifications, and has analyzed the impact of key PHY layer aspects, such as the channel model, the MCS, the relative Tx–Rx speed, and the number of occupied subchannels. In addition, the study has separately quantified the LL performance attained by the TB, first-stage SCI, and second-stage SCI transmission, which represents an important contribution to adequately model the management of radio resources at the system level.

The NR V2X SL LL performance has been analyzed by quantifying the BLER as a function of the SNR, covering the wide range of PHY and MAC layer parameters identified by 3GPP and ETSI in the default NR V2X SL parameters set. The results presented in this article demonstrate the relevant impact of the Tx–Rx relative speed, channel model, MCS, and number of subchannels on the NR V2X SL LL performance for a set of representative configurations. We should note that the trends reported in this study are in line with the observations presented in existing studies that, however, only considered a limited set of system configurations. For example, the LL results in [15], [16], and [18] have been obtained for only some of the MCSs, relative speed values, and channel models identified by 3GPP and ETSI in the default NR V2X SL parameters set. The impact of PHY layer aspects on the NR V2X SL LL performance revealed by this study highlight the importance of quantifying the LL performance under all possible system configurations. This is particularly relevant if the resulting LL models, e.g., LUTs that represent BLER versus SNR curves, are utilized to model the PHY layer effects in NR V2X SL system level studies. In order to improve the accuracy and extend the scope of system level investigations, this article openly releases to the community the complete set of BLER versus SNR curves obtained for all possible combinations of settings recommended by 3GPP and ETSI in the default NR V2X SL parameters set (i.e., a total of 1904 curves). These BLER versus SNR curves can be easily integrated into any system level or network simulator to accurately account for the impact of the PHY layer at the system level. The exhaustive set of LL results released with this article fosters the development of a common evaluation framework, providing the community with a valuable tool to accurately evaluate and fairly compare NR V2X SL communications at the system level over an exhaustive set of configurations. The data set of BLER versus SNR curves released with this article facilitates the reproducibility of the results and a direct comparison among different NR V2X SL studies that leverage our LL results.

References

[1] "Study of spectrum needs for safety related intelligent transportation systems—Day 1 and advanced use cases," 5GAA, Munich, Germany, Rep. TR-S-200137, Jun. 2020.

[2] *5G; Service Requirements for Enhanced V2X Scenarios, (Release 16), Version 16.2.0*, 3GPP Standard TS 22.186, Nov. 2020.

[3] M. H. C. Garcia et al., "A tutorial on 5G NR V2X communications," *IEEE Commun. Surveys Tuts.*, vol. 23, no. 3, pp. 1972–2026, 3rd Quart., 2021.

[4] J. Gozalvez, M. Sepulcre, and R. Bauza, "Impact of the radio channel modelling on the performance of VANET communication protocols," *Telecommun. Syst.*, vol. 50, pp. 149–167, Jul. 2012.

[5] "Github repository of the MATLAB-based NR V2X SL link level simulator." Accessed: Apr. 14, 2024. [Online]. Available: https://github.com/uwicore/NR-V2X-SL-LinkLevelSimulator

[6] "Study on evaluation methodology of new vehicle-to-everything (V2X) use cases for LTE and NR (Release 15), Version 15.3.0," 3GPP, Sophia Antipolis, France, Rep. TR 37.885, June 2019.

[7] "Intelligent transport systems (ITS); LTE-V2X and NR-V2X access layer specification for intelligent transport systems operating in the 5 GHzfrequency band; (Release 2) Version 1.1.8," ETSI Sophia Antipolis, France, Rep. EN-303 798, May 2022.

[8] "Open-source repository with the NR V2X SL link level results." Accessed: Apr. 14, 2024. [Online]. Available: https://uwicore.umh.es/NRV2XSL-LinkLevel.html

[9] W. Anwar, N. Franchi, and G. Fettweis, "Physical layer evaluation of V2X communications Technologies: 5G NR-V2X, LTE-V2X, IEEE 802.11bd, and IEEE 802.11p," in *Proc. IEEE 90th Veh. Technol. Conf.*, 2019, pp. 1–7.

[10] D. Wang, R. R. Sattiraju, A. Qiu, S. Partani, and H. D. Schotten, "Methodologies of link-level simulator and system-level simulator for C-V2X communication," in *Proc. IEEE 2nd Int. Conf. Electron. Commun. Eng. (ICECE)*, 2019, pp. 178–184.

[11] S.-Y. Lien et al., "3GPP NR sidelink transmissions toward 5G V2X," *IEEE Access*, vol. 8, pp. 35368–35382, 2020.

[12] T. Dominguez-Bolano, J. Rodriguez-Pineiro, J. A. Garcia-Naya, and L. Castedo, "The GTEC 5G link-level simulator," in *Proc. 1st Int. Workshop Link Syst. Level Simul. (IWSLS)*, 2016, pp. 1–6.

[13] S. Pratschner et al., "Versatile mobile communications simulation: The Vienna 5G link level simulator," *EURASIP J. Wireless Commun. Netw.*, vol. 2018, pp. 1–17, Sep. 2018.

[14] P. Liu et al., "Towards 5G new radio sidelink communications: A versatile link-level simulator and performance evaluation," *Comput. Commun.*, vol. 208, pp. 231–243, Aug. 2023.

[15] "Sidelink physical layer structure for NR V2X," 3GPP, Gothenberg, Sweden, document TSG, RAN WG1 Meeting #99, 3GPP R1-1911882, Nov. 2019. [Online]. Available: https://www.3gpp.org/ftp/TSG_RAN/WG1_RL1/TSGR1_99/Docs/R1-1911882.zip

[16] "Link level evaluations of NR PSSCH," 3GPP, Gothenberg, Sweden, document TSG, RAN WG1 Meeting #96, 3GPP R1-1903181, Mar. 2019. [Online]. Available: https://www.3gpp.org/ftp/TSG_RAN/WG1_RL1/TSGR1_96/Docs/R1-1903181.zip

[17] "Link level evaluations of NR PSCCH," 3GPP, Gothenberg, Sweden, document TSG, RAN WG1 Meeting #96, 3GPP R1-1903180, Mar. 2019. [Online]. Available: https://www.3gpp.org/ftp/TSG_RAN/WG1_RL1/TSGR1_96/Docs/R1-1903180.zip

[18] "Link level evaluations on sidelink for NR V2X," 3GPP, Gothenberg, Sweden, document TSG, RAN WG1 Ad-Hoc Meeting 1901, 3GPP R1-1900852, Jan. 2019. [Online]. Available: https://www.3gpp.org/ftp/TSG_RAN/WG1_RL1/TSGR1_AH/NR_AH_1901/Docs/R1-1900852.zip

[19] N. Patriciello, S. Lagen, B. Bojovic, and L. Giupponi, "An E2E simulator for 5G NR networks," *Simulat. Model. Pract. Theory*, vol. 96, Nov. 2019, Art. no. 101933.

[20] Z. Ali, S. Lagén, L. Giupponi, and R. Rouil, "3GPP NR V2X mode 2: Overview, models and system-level evaluation," *IEEE Access*, vol. 9, pp. 89554–89579, 2021.
[21] S. Lagen, K. Wanuga, H. Elkotby, S. Goyal, N. Patriciello, and L. Giupponi, "New radio physical layer abstraction for system-level simulations of 5G networks," in *Proc. IEEE Int. Conf. Commun. (ICC)*, 2020, pp. 1–7.
[22] L. Lusvarghi and M. L. Merani, "MoReV2X—A new radio vehicular communication module for ns-3," in *Proc. IEEE 94th Veh. Technol. Conf.*, 2021, pp. 1–7.
[23] A. Molina-Galan, B. Coll-Perales, L. Lusvarghi, J. Gozalvez, and M. L. Merani, "How does 5G NR V2X mode 2 handle aperiodic packets and variable packet sizes?" in *Proc. IEEE 23rd Int. Conf. High Perform. Switch. Rout. (HPSR)*, 2022, pp. 183–188.
[24] *NR; User Equipment (UE) Radio Transmission and Reception; Part 1: Range 1 Standalone (Release 17)*, 3GPP Standard TS 38.101-1, Mar. 2021.
[25] *NR; Multiplexing and Channel Coding, (Release 16), Version 16.5.0*, 3GPP Standard TS 38.212, Mar. 2021.
[26] *NR; Physical Layer Procedures for Data, (Release 16), Version 16.5.0*, 3GPP Standard TS 38.214, Mar. 2021.
[27] *NR; Physical Channels and Modulation, (Release 16), Version 16.5.0*, 3GPP Standard TS 38.211, Mar. 2021.
[28] "Release 16 description; summary of rel-16 work items, (Release 16), Version 0.6.0," Sophia Antipolis, France, Rep. 21.916, Sep. 2020.
[29] I. Tal and A. Vardy, "List decoding of polar codes," *IEEE Trans. Inf. Theory*, vol. 61, no. 5, pp. 2213–2226, May 2015.
[30] *NR; Medium Access Control (MAC) Protocol Specification, (Release 16), Version 16.4.0*, 3GPP Standard TS 38.321, Mar. 2021.

Luca Lusvarghi (Associate Member, IEEE) received the master's degree (summa cum laude) in electronics engineering and the Ph.D. degree in information and communication technology from the University of Modena and Reggio Emilia, Modena, Italy, in 2019 and 2023, respectively.

He is currently a Postdoctoral Researcher with the UWICORE Laboratory, Universidad Miguel Hernández de Elche, Elche, Spain. His research interests include cooperative, connected and automated mobility, vehicle-to-everything communications, AI-based 6G wireless communications, and semantic communications.

Dr. Lusvarghi was the recipient of the Vetrya Award for the Best Italian Master's Degree Thesis on 5G and of the GTTI Ph.D. Award for the Best Italian Ph.D. Thesis in ICT.

Baldomero Coll-Perales (Member, IEEE) received the M.Sc. and Ph.D. degrees in telecommunications engineering from the Universidad Miguel Hernández de Elche (UMH), Elche, Spain, in 2008 and 2015, respectively.

He is an Associate Professor with UMH, Spain. He has held Senior Research Fellow (Ramón y Cajal, Juan de la Cierva) positions with the UWICORE Laboratory, UMH. He has held Visiting Research positions with the Universidad Politécnica de Cartagena, Cartagena, Spain; Hyundai Motor Europe Technical Center, Main, Germany; Italian National Research Council, Rome, Italy; Rutgers University Wireless Information Network Laboratory, North Brunswick Township, NJ, USA; and the Institute of Telecommunications, King's College London, London, U.K. His research interests lie in the field of advanced mobile and wireless communication systems applied towards the digitalization of critical verticals, with relevant contributions in 6G/5G and beyond 5G, connected and automated driving, and Industry 4.0.

Dr. Coll-Perales serves/has served as an Associate Editor for the *International Journal of Sensor Networks* and *Telecommunication Systems* (Springer). He has served as a Track Co-Chair for IEEE VTC-Fall 2018 and as a member for TPC in over 45 international conferences.

Javier Gozalvez (Senior Member, IEEE) received the electronics engineering degree from the Engineering School, ENSEIRB, Bordeaux, France, in 1998, and the Ph.D. degree in mobile communications from the University of Strathclyde, Glasgow, U.K., in 2002.

He is a Full Professor with the Universidad Miguel Hernández de Elche, Elche, Spain, where he leads research activities in the areas of vehicular networks, 5G and beyond, and industrial wireless networks.

Prof. Gozalvez is the Editor in Chief of the *IEEE Vehicular Technology Magazine*. He is a Scientific Evaluator and a reviewer for the European Commission and various national scientific and technical agencies. He is an Elected Member to the Board of Governors of the IEEE Vehicular Technology Society (IEEE VTS) and was the 2016 and 2017 President of the IEEE VTS. He has served as an IEEE Distinguished Speaker and an IEEE Distinguished Lecturer for the IEEE VTS.

Maria Luisa Merani (Senior Member, IEEE) received the Ph.D. degree from the University of Bologna, Bologna, Italy, in 1992.

In 1991, she was a Visiting Researcher with the University of California at Los Angeles, Los Angeles, CA, USA. She is currently an Associate Professor with the Department of Engineering "Enzo Ferrari," University of Modena and Reggio Emilia, Modena, Italy. She is also an Associate Member of the Consorzio Nazionale Interuniversitario per le Telecomunicazioni, Parma, Italy. Her research interests include wireless networking, with emphasis on 5G/6G vehicular communications, safety of road users, and performance analysis of radio access techniques.

Dr. Merani served as an Editor for the IEEE TRANSACTIONS ON WIRELESS COMMUNICATIONS.